The International Journal of Advanced Manufacturing Technology
https://doi.org/10.1007/s00170-019-04875-9

ORIGINAL ARTICLE

Performance evaluation of a giant magnetostrictive rotary ultrasonic machine tool

Huilin Zhou[1] · Jianfu Zhang[1,2,3] · Pingfa Feng[1,2,3] · Dingwen Yu[1] · Wanchong Cai[1] · Jianjian Wang[4]

Received: 14 July 2019 / Accepted: 19 December 2019

Abstract
A giant magnetostrictive rotary ultrasonic machine tool (GMRUMT) with a large and stable amplitude output was developed. The purpose of this study was to comprehensively evaluate the performance and technological characteristics of the GMRUMT by conducting large amplitude experiments of rotary ultrasonic machining. Combined with the transducers' characteristic curves of vibration amplitude versus frequency, the GMRUMT has the advantages of greater amplitude, higher power, and better stability compared with the conventional piezoelectric actuated rotary ultrasonic machine tool. The vibration stability of the GMRUMT during the machining process was evaluated by carrying out the rotary ultrasonic face milling of quartz glass and the measurement of the actual ultrasonic amplitude. The processing performance of the GMRUMT was evaluated by obtaining the cutting force, the critical feed rate, and the edge-chipping size at the exit hole via rotary ultrasonic drilling experiments. The tool life was evaluated by observing the abrasive wear of the tool. Finally, the GMRUMT was studied in a stable amplitude output condition via tuning to verify the machining advantages of the GMRUMT.

Keywords Giant magnetostrictive rotary ultrasonic machine tool · Vibration amplitude · Cutting force · Edge chipping · Abrasive wear

1 Introduction

With the vigorous development of high-tech industry, there is a greater demand for structural materials in the fields of aerospace, automobile manufacturing, medical devices, and nuclear energy [1–3]. Brittle materials have been extensively applied to these industries, which include optical glass [4, 5], advanced ceramics [6], and ceramic matrix composites [7], which are characterized by high hardness, good wear resistance, and corrosion resistance [8]. However, due to their high hardness and low fracture toughness, brittle materials have become difficult to machine, which has made efficient precision machining a research hotspot [9].

In order to reduce production costs and improve production efficiency, after years of research, a variety of mechanical machining methods for brittle materials have emerged, including diamond grinding [10], laser machining [11], electrical discharge machining [12], ultrasonic machining [13], ultrasonic-vibration-assisted grinding [14], ultrasonic-vibration-assisted filing [15], and rotary ultrasonic machining (RUM) [16, 17]. It has been determined that dynamic intermittent machining resulting from ultrasonic vibration has become an effective way to process brittle materials.

Many experimental studies have demonstrated that utilizing RUM in brittle materials machining can effectively improve machining efficiency and machining quality, and can extend the tool's life [18, 19]. Due to the brittleness of materials, edge chipping, especially at the exit hole, occurs in the hole machining of brittle materials, and seriously reduces the accuracy and the service life of machined parts; it has therefore become one of the key problems in the machining of brittle materials [20]. As shown in Fig. 1, RUM combines the axial feed motion, the axial ultrasonic vibration, and the

✉ Jianfu Zhang
zhjf@tsinghua.edu.cn

[1] State Key Laboratory of Tribology, Department of Mechanical Engineering, Tsinghua University, Beijing 100084, China

[2] Beijing Key Lab of Precision/Ultra-precision Manufacturing Equipments and Control, Department of Mechanical Engineering, Tsinghua University, Beijing 100084, China

[3] Division of Advanced Manufacturing, Graduate School at Shenzhen, Tsinghua University, Shenzhen 518055, China

[4] Department of Mechanical Engineering and Automation, The Chinese University of Hong Kong, Hong Kong, China

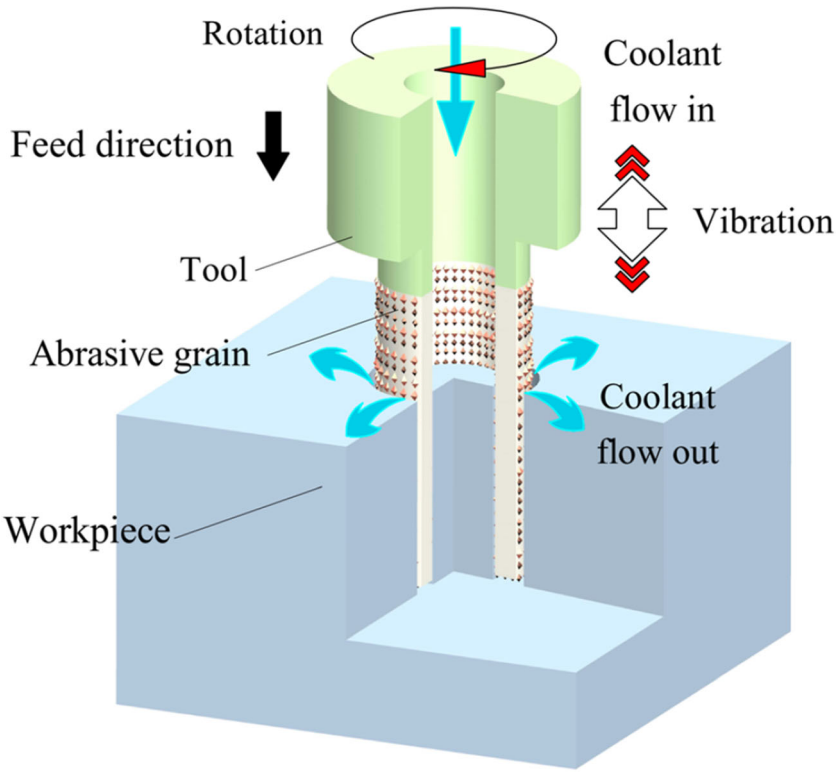

Fig. 1 Schematic diagram of rotary ultrasonic drilling

spindle rotation motion. In order to remove materials, the hollow tool is adhered to diamond or cubic boron nitride (CBN) via sintering, electroplating, or brazing. It is then cooled by the coolant, and the chips are removed during processing.

Due to the limitation of the development of functional materials, the research on the RUM of brittle materials was mainly conducted on ultrasonic machine tools with $Pb[Zr_xTi_{1-x}]O_3$ (PZT). In the 1970s, CLARK in the USA first proposed the rare-earth compound [21] with giant magnetostrictive properties, which resulted in the availability of giant magnetostrictive material (GMM). The GMM, represented by Terfenol-D, has the advantages of giant magnetostriction (over 1000 ppm), fast response speed, and high energy density [22], which have allowed for its successful application in actuators, transducers, and motors [23]. Therefore, through reasonable structural design, it is possible to develop a giant magnetostrictive ultrasonic transducer (GMUT) that is characterized by a large amplitude output and high power. Developing a novel giant magnetostrictive rotary ultrasonic machine tool (GMRUMT) with GMUT as an ultrasonic oscillator will be very meaningful for the development of RUM technology. Due to the problems of temperature change, load impact, and frequency drift in machining, there are few reports on the practical application of GMUT in RUM machine tools.

Based on previous research [24–26], this study proposes a GMRUMT with a large and stable amplitude output for the first time. Combined with the amplitude–frequency characteristic curve, the actual ultrasonic amplitude was measured through rotary ultrasonic face milling experiments of quartz glass to analyze the equipment performance of the GMRUMT, and the machining quality was evaluated using rotary ultrasonic drilling experiments of quartz glass to verify the machining advantages of the GMRUMT. This study aims to comprehensively test the performance of the GMRUMT and evaluate its technological characteristics by carrying out large amplitude RUM experiments.

2 Development of giant magnetostrictive rotary ultrasonic machine tool

2.1 Giant magnetostrictive ultrasonic transducer

The PZT transducer and the GMUT are illustrated in Fig. 2. The GMUT consists of a screw bolt, front cover plate, rear cover plate, GMM, horn, and excitation circuit. Acting on the GMM installed on the central axis, the front cover plate and the rear cover plate produce prestress with the action of prestress bolts. The alternating magnetic field is generated by the alternating current signal through the excitation circuit, which drives the GMM to produce ultrasonic strain along the axis. The horn is connected with the front cover plate to realize the transmission and amplification of ultrasonic vibration.

The external diameter, internal diameter, and thickness of the PZT are ∅50 mm, ∅15 mm, and 6.5 mm, respectively, and

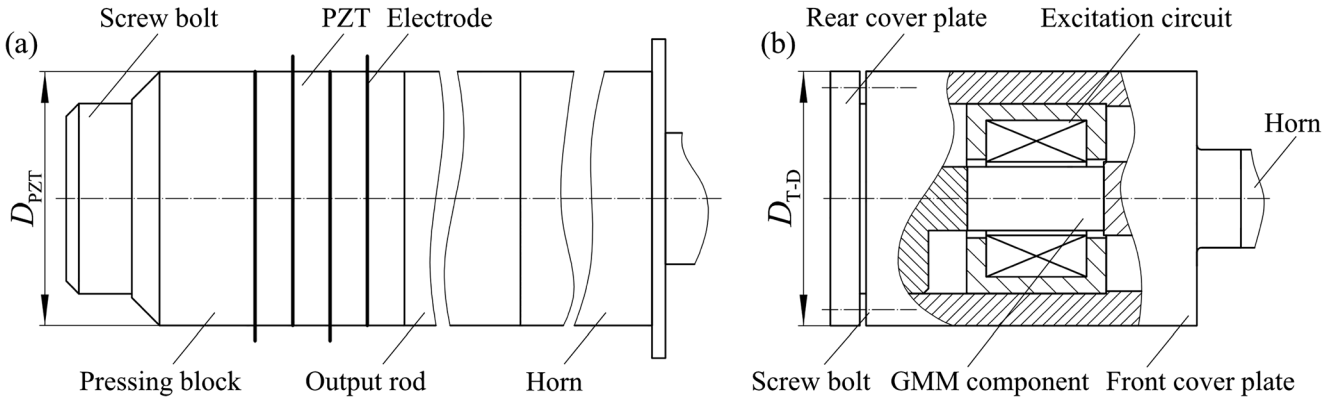

Fig. 2 Structural diagrams of **a** the PZT transducer and **b** the GMUT

the size of the GMM component is ∅13 × 27.8 mm, as shown in Fig. 3. Due to the characteristics of the GMM, the GMM component is sliced into 13 equal-width portions to minimize the eddy current effect. In Fig. 3, the GMM component consists of two GMMs with slice processing, three permanent magnets, and two silicon steels connected by epoxy resin. And the permanent magnets are used to increase the static magnetic field and avoid the frequency doubling effect, and the silicon steel used for magnetic conduction is also sliced.

In order to quantitatively characterize the amplitude stability, the effective frequency bandwidth Δf was defined as the two frequency differences when the amplitude reaches $\frac{\sqrt{2}}{2}A_n$, where A_n represents the resonant amplitude, and Δf is obtained by interpolation. Figure 4 presents the amplitude–frequency characteristic curves of the PZT transducer [27] and the GMUT almost at the same scale. The electrical characteristics of the PZT transducer consist of conductance and admittance, and those of the GMUT consist of resistance and reactance. They are reciprocal; therefore, whether constant voltage excitation or constant current excitation is used, different relation curves of the current and voltage versus excitation frequencies will be obtained. Thus, when a constant input power is used for excitation, the current and voltage variation of the two systems under different excitation frequencies will become non-deterministic due to the different working principles of the ultrasonic power supply used in the experiments. This is the reason why the input power was not used to compare the performance of the two kinds of transducers. In addition, the amplitude output of the PZT transducer and the GMUT are caused by voltage and current, respectively, so it is difficult to reach a unified conclusion when the working principles of the selected ultrasonic power supply are uncertain. Therefore, performance comparison under a constant voltage mode was used to express the advantages of the GMUT compared with the PZT transducer in amplitude stability under the same excitation voltage amplitude.

Table 1 provides the structural and experimental parameters in detail for the amplitude–frequency characteristic curves of the two transducers. Compared with the PZT transducer, it can be seen that under the same excitation voltage, the resonance frequencies of both kinds of transducers are similar (20 kHz ± 500 Hz), but the resonance amplitude of the GMUT is much larger than that of the PZT transducer, and the corresponding effective frequency bandwidth Δf is much larger than that of the PZT transducer (about 8.32 times), which means that the amplitude–frequency characteristic curve of the GMUT is more "gentle." Therefore, when the resonance state is affected by external interference, the amplitude attenuation of the GMUT is smaller, which means exhibiting better amplitude stability.

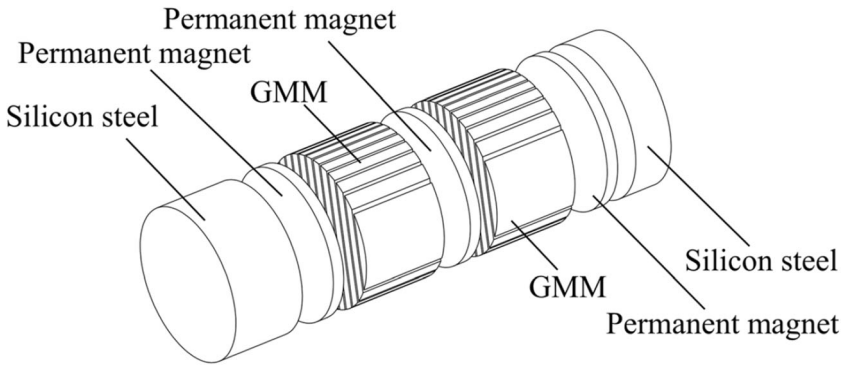

Fig. 3 Structural schematic diagram of the GMM component

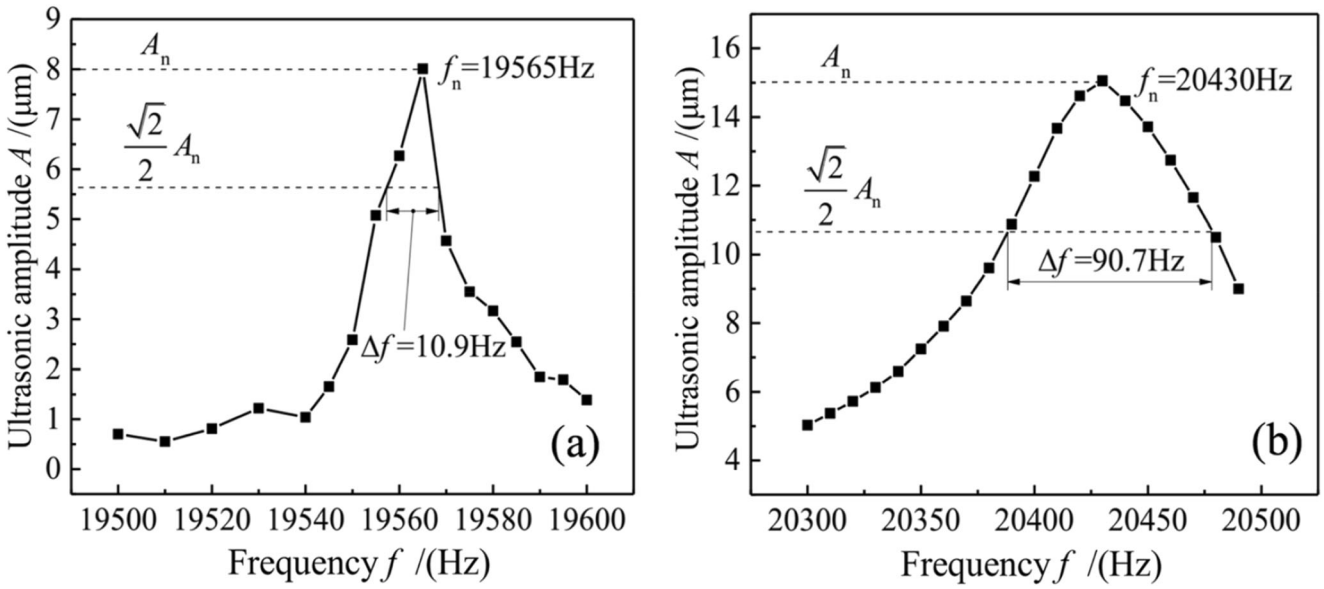

Fig. 4 Amplitude–frequency characteristic curves of **a** the PZT transducer [27] and **b** the GMUT

2.2 Rotary ultrasonic machine tool

In this study, a GMRUMT called the THU ULTRASONIC 850 was developed as shown in Fig. 5. The BP4610 ultrasonic power supply outputs a signal to the GMUT through the energy transfer mechanism. Due to the coil structure in the GMUT, the circuit is inductive under no compensation. Therefore, the compensation circuit plays a role in compensating the circuit, which means that the compensation of capacitance results in the pure resistance of the circuit, i.e., the reactance is 0. The impedance circle is symmetrical about the abscissa, and the point with a reactance of 0 can be better determined by the change of the acquired electrical signal. An oscilloscope (MDO3041) was used to monitor the voltage and current signal in real time. The computer acquired data using a dynamometer (Kistler 9256C2), on which the workpiece was fixed through the lock block and fixture at a sampling frequency of 1000 Hz.

In order to determine the resonant amplitudes under different excitation voltages, a laser displacement sensor (LKH008, Keyence, Japan) was used to measure the ultrasonic amplitude at the end of the tool. The maximum sampling frequency could be as high as 392 kHz, and the resolution was 0.1μm (as shown in Fig. 6). If not specified, the ultrasonic amplitude refers to the idling amplitude, i.e., the amplitude under a no-load condition.

The change of the vibration amplitude with time at an excitation voltage amplitude of 25 V is presented in Fig. 7. The frequency sweeping experiment was conducted at frequencies from 20,240 Hz to 20,620 Hz, the increment was 20 Hz, the step time was 0.07 s, and the abscissa represents the number of data points; one sampling point represents approximately 5 μs because the sampling frequency of the laser displacement sensor was 200 kHz. It can be seen that the total excitation time was only 1.4 s, and the collected waveform was relatively stable during the process of determining the resonant amplitude.

The main technical parameters of the GMRUMT are listed in Table 2. A central air-cooling system consisting of an air compressor, gas container, and cooler was designed on the spindle of the GMRUMT according to the characteristics of the GMUT and the installation requirements of the holder to realize RUM.

The large amplitude ultrasonic vibration is caused by the excitation of the large current, and the generated heat will cause thermal deformation and affect the machining accuracy. In order to solve this problem, the air cooling method was used. In the designed GMUT, the cooling air

Table 1 The structural and experimental parameters in detail for the amplitude–frequency characteristic curves

Functional material	Excitation voltage amplitude (V)	External diameter of transducer (mm)	Resonance amplitude (μm)	Trend of curve
PZT	30	D_{PZT}=50	8	Sharp
GMM		D_{T-D}=52	15	Gentle

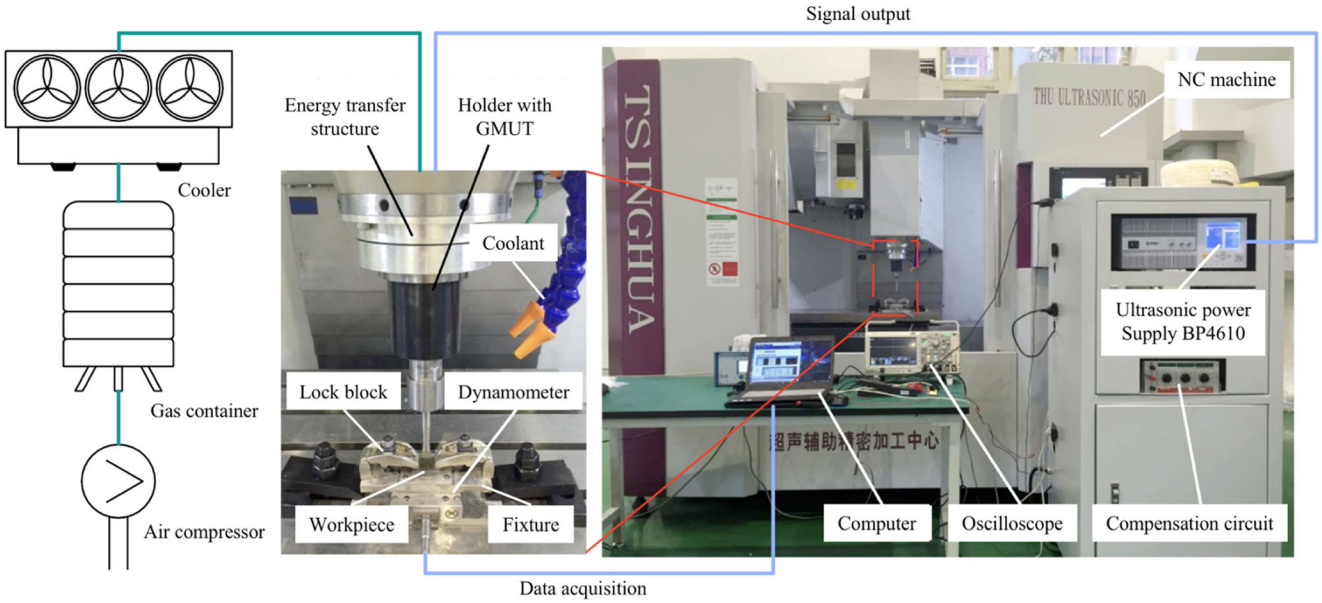

Fig. 5 Structural schematic diagram of the GMRUMT

flows around the GMM component, and the air gap is sufficiently narrow, resulting in a large air velocity. The temperature measurement experiments conducted before the experiment demonstrate that under the excitation of the largest excitation voltage amplitude that can be realized by the ultrasonic power supply (60 V), the temperature can be stabilized at the thermal balance temperature (at the surface of the GMM, around 30 °C) in up to 3 min. Therefore, air cooling was conducted for 3 min before all experiments to minimize the impact of

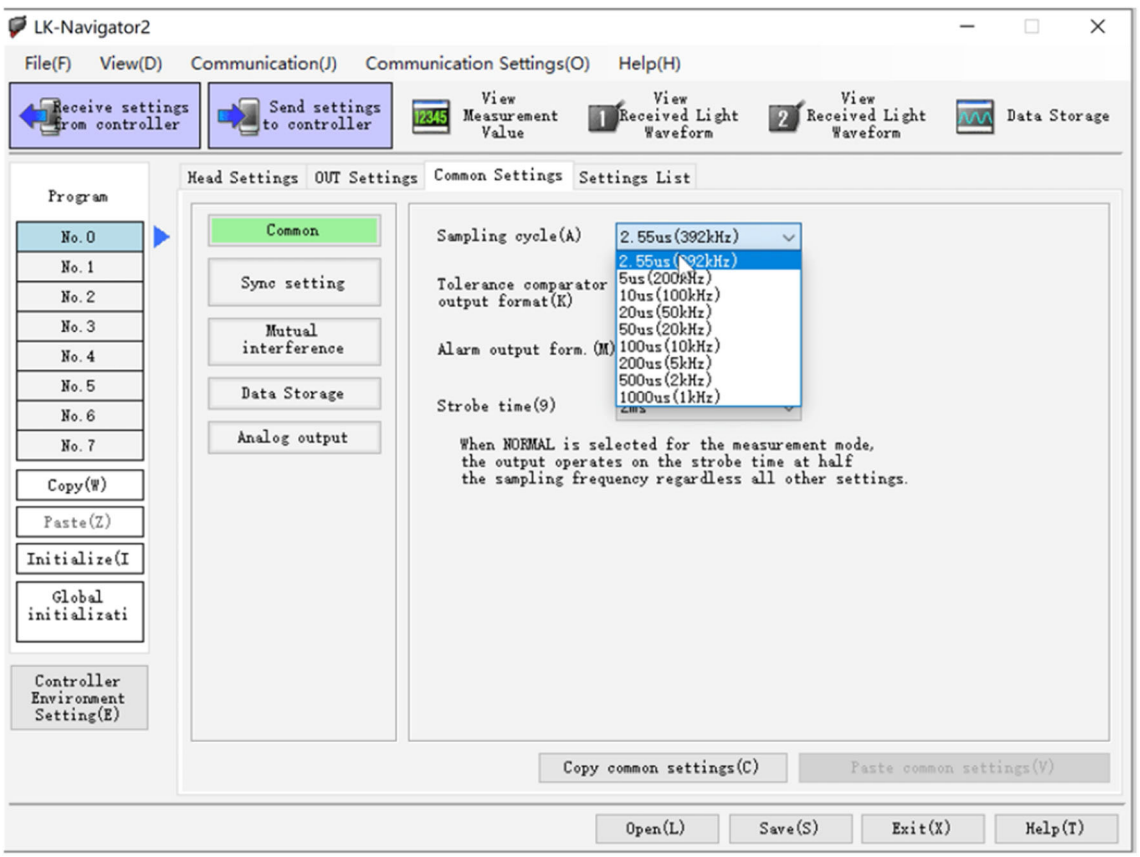

Fig. 6 The optional sampling frequencies of the laser displacement sensor

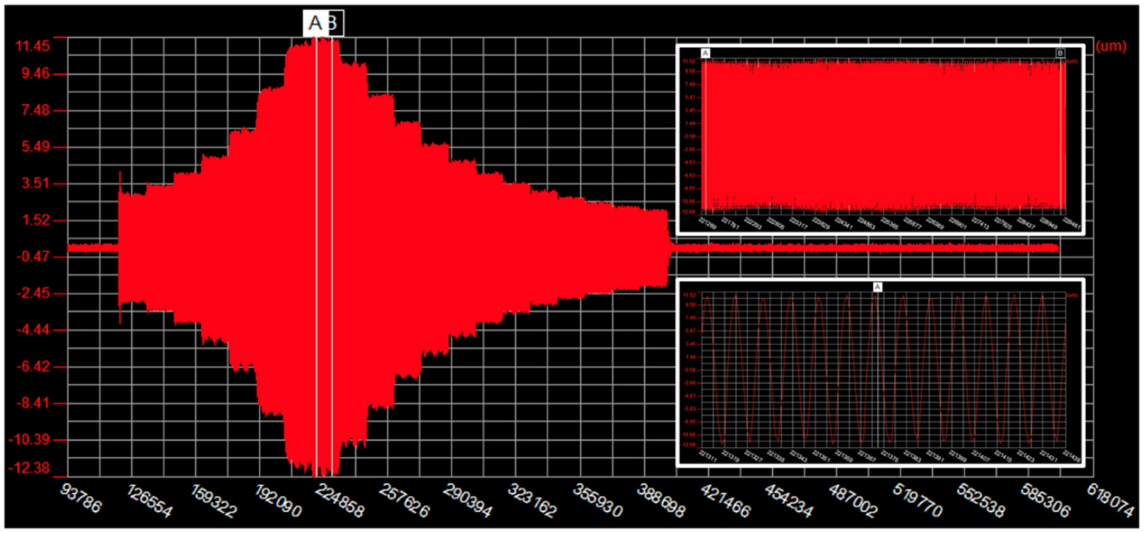

Fig. 7 The measurement result of the vibration amplitude with time (Excitation voltage amplitude: 25 V)

temperature rise. In order to reduce the influence of the thermal elongation of the horn, coolant was added to cool the working area. Additionally, the material removal time was minimized to minimize the influence of temperature rise in the process of cutting experiment.

3 Experimental design of processing performance evaluation

3.1 Rotary ultrasonic face milling

To test the equipment performance of the GMRUMT, the influence of the cutting depth on the cutting force was explored through the rotary ultrasonic face milling experiments to avoid the excessive cutting force caused by the improper workpiece from suppressing the ultrasonic action, and ensure the smooth development of the experiments. And the relationship between the attenuation of the actual ultrasonic amplitude and the cutting depth under different excitation voltages by using the proposed calculation method was also explored. For the rotary ultrasonic face milling, the advantages of large amplitude rotary ultrasonic machining can be highlighted in machining difficult-to-machine materials with high hardness and high wear resistance, such as SiCp/Al composites [28]; however, guaranteeing the surface quality is difficult, and the overall cutting force in the cutting process may be large, which is not conducive to the development of experiments. Thus, the quartz glass was selected as the workpiece for relatively low hardness and wear resistance. The experimental parameters of the equipment performance tests are presented in Table 3. The system for the GMRUMT was operated under three excitation voltages. The spindle speed and feed rate were set to 2000 r/min and 80 mm/min, respectively. The workpiece size was 40 × 60 × 8 mm. By

Table 2 Technical parameters of the THU ULTRASONIC 850

Item		Unit	Value
Stroke	X-stroke	mm	850
	Y-stroke	mm	550
	Z-stroke	mm	540
Spindle	Maximum spindle speed	r/min	10,000
	Standard for taper of spindle hole	-	BT-40
Accuracy (Linear axis accuracy referring to standard JB/T8772.4-1998)	Positioning accuracy	mm	0.018
	Repetitive positioning accuracy	mm	0.012
NC system		-	Siemens840D
Ultrasonic system	Excitation frequency	kHz	18–30
	Ultrasonic power	W	200–400
	Vibration amplitude	μm	8–27
Air cooling system	Pressure	MPa	0–0.8

Table 3 Experimental parameters of rotary ultrasonic face milling experiments

Experiment	Amplitude of excitation voltage (V)	Idling amplitude A_I (μm)	Resonant frequency f (Hz)	Cutting depth τ (μm)
Group 1	25	12	20,370	0, 50, 100, 150, 200, 250, 300
Group 2	35	18	20,360	
Group 3	45	24	20,350	

changing the excitation frequency, the amplitude–frequency characteristic curves were obtained, and the resonance frequency was also determined.

The experimental sketch of the rotary ultrasonic face milling experiments is shown in Fig. 8. The excitation frequency was set to the resonance frequency of the GMRUMT under a no-load condition. In face milling, the cutting depth refers to the vertical distance between the machined surface and the surface to be machined, thus the actual cutting depth τ' is the sum of the theoretical cutting depth τ and the actual ultrasonic amplitude A'due to the ultrasonic vibration. When the tool completed half of the processing of the quartz glass, the ultrasonic power was turned off, which meant that the actual cutting depth changed to the theoretical cutting depth τ set in the numerical control (NC) program; thus, a small step remained on the workpiece surface. After machining, in order to avoid the influence caused by the crushing of the brittle edge of the quartz glass to the greatest extent, a large spindle speed and low feed rate were implemented, and a micrometer was utilized to measure the minimum height among the multiple points at the two measured step surfaces, which represented the actual ultrasonic amplitude.

3.2 Rotary ultrasonic drilling

To study the influences of the ultrasonic amplitude, feed rate, and tuning on the RUM of brittle materials, four amplitudes (0 μm, 12 μm, 18 μm, and 24 μm, where 0 μm represents no ultrasonic excitation, i.e., traditional drilling) were selected to carry out the rotary ultrasonic drilling experiments on quartz glass. The experimental parameters for the process performance tests are listed in Table 4, and the spindle speed was set to 2000 r/min. The workpiece size was 40 × 40 × 5 mm. The experiments were carried out with different feed rates. The cutting force and the edge-chipping size in the process were measured. Additionally, the cutting force in this study refers to the z-direction cutting force.

The tool life is related to the abrasive wear. Reducing the tool wear is helpful for reducing the machining cost and improving the stability of the machining process. In order to study the influence of ultrasonic amplitude on the wear process of diamond tools, four diamond tools adhered to the same abrasive grain size (about 100 μm) were selected to carry out the tool wear experiments on quartz glass with the same machining parameters under the four different ultrasonic

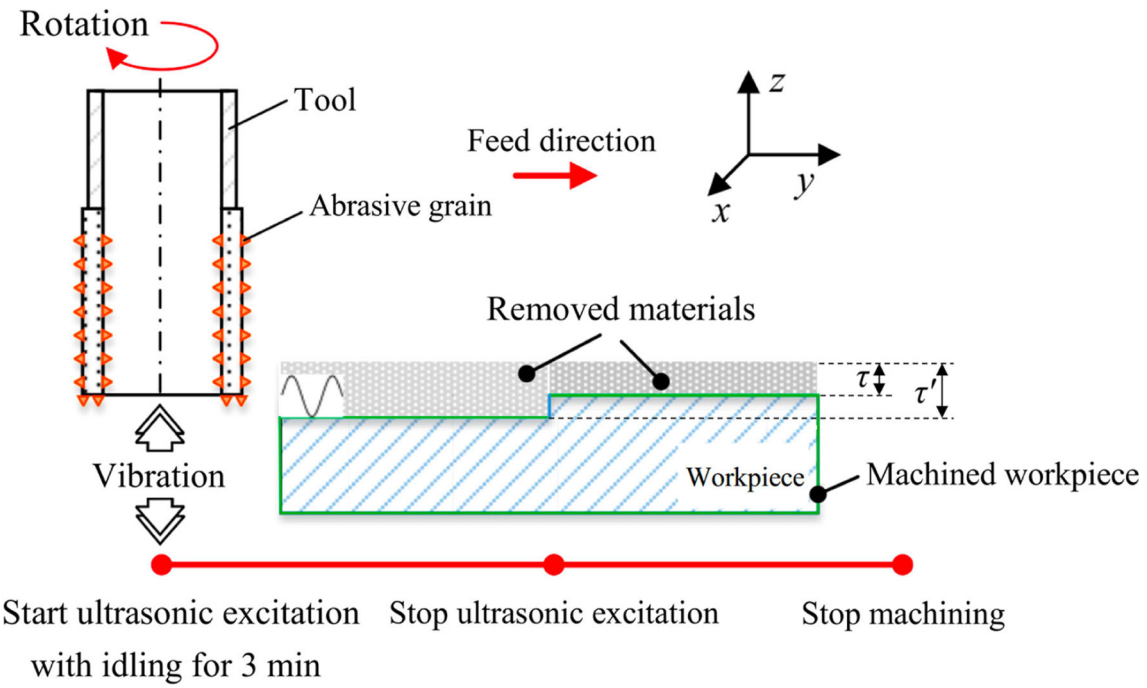

Fig. 8 Experimental sketch of rotary ultrasonic face milling experiments

Table 4 Experimental parameters of rotary ultrasonic drilling experiments

Experiment	Idling amplitude A_I (μm)	Feed rate v_f (mm/min)	Ultrasonic excitation	Tuning
Group 1	12	1, 2, 3, 4, 5, 6	✓	✗
Group 2	12	1, 2	✓	✓
Group 3	12	1, 2, 3, 4	✗	✗
Group 4	18	1, 2, 3, 4, 5, 6	✓	✗
Group 5	18	1, 2	✓	✓
Group 6	18	1, 2, 3, 4	✗	✗
Group 7	24	1, 2, 3, 4, 5, 6	✓	✗
Group 8	24	1, 2	✓	✓
Group 9	24	1, 2, 3, 4	✗	✗

amplitudes. The experimental parameters are exhibited in Table 5. The workpiece size was 80 × 40 × 8 mm Holes were made at equal spacing on the workpiece. Cutting forces were collected in real time, and the average cutting forces were then calculated during the process of single hole drilling. The relationship curve between the average cutting forces and the number of holes was established.

3.3 Measurement method of processing outputs

3.3.1 Measurement method for the actual ultrasonic amplitude

The measurement schematic diagram of the actual ultrasonic amplitude is illustrated in Fig. 9. The feed direction was perpendicular to the direction of ultrasonic vibration. The side abrasive grains (marked in black in the figure) played a major role in the cutting process. Because the vibration direction of the GMRUMT was axial, i.e., in the z-direction, the axial load significantly affected the change of vibration performance. However, most of the end abrasive grains only vibrated on the machined plane, which meant that the axial load of the ultrasonic system was small. Therefore, the mechanical loads during plane machining had little influence on the vibration performance of the GMRUMT in the z-direction.

It should be noted that with the increase in cutting depth, more side abrasive grains were involved in the machining, while the end abrasive grains machined the plane based on the side abrasive grains. If factors such as tool deformation and workpiece surface topography are neglected, the actual cutting depth τ' in plane machining should be the sum of the theoretical cutting depth τ and the actual ultrasonic amplitude A'. We therefore obtain

$$A' = \tau' - \tau \tag{1}$$

During the rotary ultrasonic face milling experiments, the GMRUMT only produced large amplitude ultrasonic vibration in the z-direction, which means that the ultrasonic vibration direction was perpendicular to the feed direction, and the side abrasive grains played a major role in the cutting process. The cutting depth range was 0–300 μm, and the ultrasonic amplitude range was 12 μm–24 μm, ; thus, the cutting depth had a larger influence on the contact area between the side abrasive grains and the workpiece. Additionally, the feed rate can increase the contact time between the side abrasive grains and the workpiece; therefore, the processing parameters, such as the cutting depth and feed rate, may have the greater impacts on the cutting forces in the x- and y-directions, which means that the cutting forces in the x- and y-directions may have no direct relationship with the ultrasonic amplitude in the z-direction. The purpose of the rotary ultrasonic face milling experiments was to explore the advantages of a large amplitude in the cutting process, and to determine the relationship among the attenuation of the ultrasonic amplitude, the increase in the cutting force, and the cutting depth. Therefore, the forces in the x- and y-directions are not discussed in the present work Due to the limited sampling frequency of the Kistler 9256C2 dynamometer, the curve of cutting force measurement consisted of several discrete points. In order to effectively evaluate the cutting force, the average cutting force was utilized as the calculation index in this study, as given in Eq. (2):

$$F_z = \frac{1}{m}\sum_{i=1}^{m} F_i \tag{2}$$

where F_z denotes the average cutting force in the z-direction, m is the number of cutting force data points collected from the beginning of machining to the end of machining, and F_i represents the value of each cutting force data point. It should be noted that the cutting force curve should be drift compensated to remove the influence caused by the zero drift of the equipment.

3.3.2 Measurement method for the machined quality

The measurement schematic diagram for the edge-chipping size at the exit hole is shown in Fig. 10. The edge-chipping size was closely related to the cutting force at the exit hole. There were two main evaluation indicators of edge-chipping damage, namely the thickness of edge chipping d_t and the

Table 5 Experimental parameters of tool wear

Tool number	1	2	3	4
Idling amplitude A_I (μm)	0	12	18	24
Thickness of tool wall (mm)	1.2			
Spindle speed (r/min)	2000			
Feed rate v_f (mm/min)	2			

width of edge chipping d_s, as shown in Fig. 10a. Considering the difficulty of measurement, the width of edge chipping d_s (half of the difference between the diameter of the enveloping line and the diameter of the hole) was used as the main index to measure the edge-chipping size. The edge-chipping sizes under different machining parameters and ultrasonic amplitudes were measured using a microscope with a super wide depth of field (VHX-600, Keyence, Japan), as shown in Fig. 10b.

3.3.3 Measurement method for the abrasive wear

To effectively and qualitatively evaluate the abrasive wear under different ultrasonic amplitudes, the experiments of tool wear under different amplitudes were conducted, and the relationship between the cutting force and the number of drilled holes were also discussed. The final surface morphologies of the four tools at the same number of machined holes (36 times) were observed by the microscope with a super wide depth of field, as shown in Fig. 10b.

4 Results and discussion of processing performance evaluation

4.1 Stability of actual ultrasonic amplitude in machining process

During the process of machining, if the actual ultrasonic amplitude stability is not sufficient, the cutting force may increase and further contribute to the decline of the quality of the machined surface. Thus, the relationship between the cutting force and the cutting depth in rotary ultrasonic face milling is presented in Fig. 11. The average cutting force according to Eq. (2) was utilized as the calculation index. To address the drift generated in cutting force measurement, the Kistler 9256C2 dynamometer instrument was compensated by itself before operation;

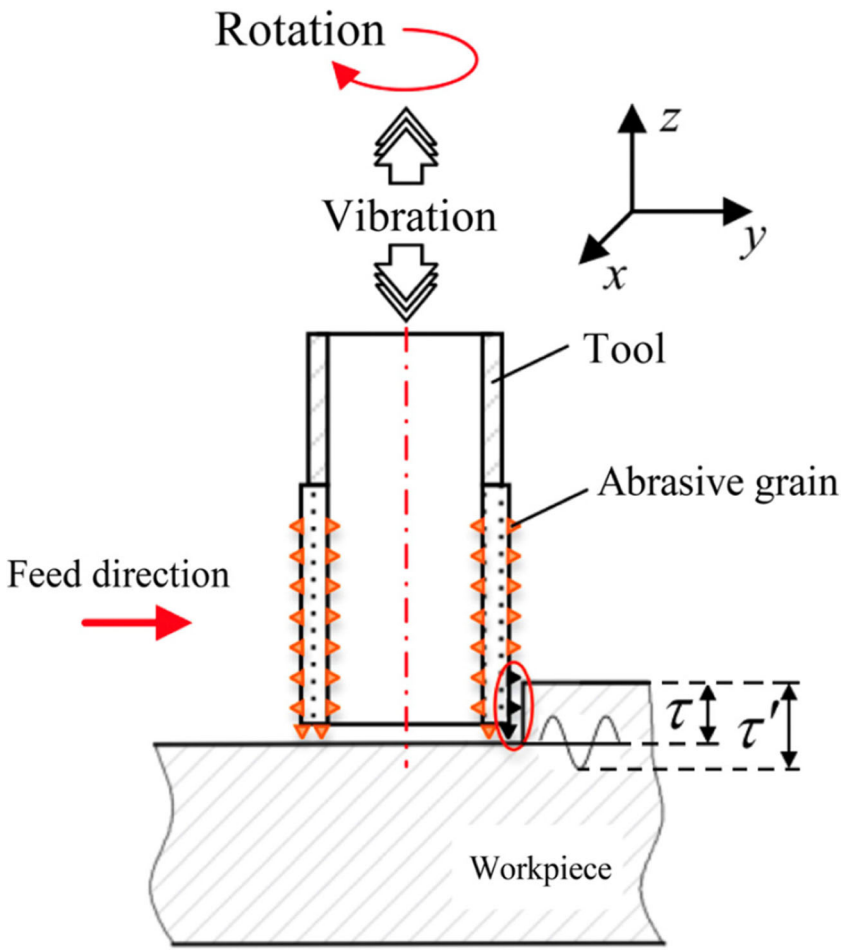

Fig. 9 Measurement schematic diagram of actual ultrasonic amplitude

however, there remained some errors in the equipment, resulting in the deviation of the collected cutting force from 0 by a small amount when it was running under no load. Therefore, to obtain the more reasonable curve of the change of the actual cutting force with time, the curves compensated via the Kistler instrument's software. From the graph, it is evident that:

1) The cutting force was generally small. This is because the side abrasive grains played a major role in material removal. Thus, the axial load acting on the GMRUMT was generally small, which made the ultrasonic vibration difficult to be suppressed;
2) The cutting force increased with the increase in cutting depth. The reason for this is that with the increase in cutting depth, the contact area between the tool and workpiece increased, as did the machining load acting on the GMRUMT This led to the resonance–frequency drift and the decrease in the actual ultrasonic amplitude, thereby increasing the cutting force;
3) When the cutting depth was far greater than the ultrasonic amplitude, the ultrasonic vibration was not invalid, which indicates that there is no direct relationship between the cutting depth and the ultrasonic amplitude. Increasing the ultrasonic amplitude can therefore effectively reduce the cutting force under certain machining parameters.

By measuring the step height on the workpiece, the actual ultrasonic amplitude of the GMRUMT in face milling was obtained, as shown in Fig. 12. From a physical perspective, the crushing of the brittle edge of the cutting zone will lead to slightly larger measurement results. In Fig. 12, it can be seen that one point of the actual ultrasonic amplitude of 35 V (18 μm) during the cutting process was larger than that under the no-load condition, which indicates that the crushing of the brittle edge must have occurred. The results demonstrate the following.

1) When the excitation voltage was large, such as 35 V or 45 V, the actual ultrasonic amplitude of the GMRUMT was stable under different cutting depths. The reason for this is that increasing the ultrasonic amplitude can effectively reduce the cutting force, thereby reducing the axial mechanical load. Therefore, the actual ultrasonic amplitude of the GMRUMT under the condition of a large amplitude was relatively stable.
2) When the excitation voltage was 45 V, the measured actual ultrasonic amplitude was larger than that under a no-load condition. The possible reasons for this are (a) when the large ultrasonic vibration impacted the workpiece surface, the crack depth on the material surface was larger, which made the removal depth greater than the actual vibration amplitude; (b) with an increase in excitation voltage, the temperature of the GMM increased which resulted in the thermal elongation of the tool. When the ultrasonic power was turned off, the ultrasonic vibration and the thermal elongation disappeared synchronously, thus the step height was greater than the actual ultrasonic amplitude. Although some error factors are included in the measured actual ultrasonic amplitude data, the data in Fig. 12 reflect the variation law of actual ultrasonic amplitude in plane machining to a certain extent.
3) Increasing the idling amplitude using a large excitation voltage can reduce the cutting force and thus decrease the mechanical load under certain machining parameters. In addition, by increasing the idling amplitude, the actual ultrasonic amplitude of the GMRUMT under a certain load can be increased.

4.2 Cutting force and critical feed rate

The critical feed rate [29] has been proposed for the performance evaluation of ultrasonic machine tools. In Fig. 13, the cutting force tended to be stable with the increase of ultrasonic amplitude. Under the amplitude of 24 μm, the cutting force was nearly stable around 7 N throughout the machining process.

The relationship between the cutting force and the machining parameters can be further obtained from Fig. 14. In the process of rotary ultrasonic drilling, the critical feed rate can be found [29]. This is because when the feed rate reaches its critical feed rate, the intermittent impact between the abrasive particles and the workpiece becomes a continuous contact effect, thereby increasing the contact area of the end face, and resulting in the rise of the cutting force in the z-direction. According to the relationship between the critical penetration depth and the actual ultrasonic amplitude, the critical feed rate in the GMRUMT can be defined as follows [30].

$$v_{\mathrm{f}}^{'} = 2A^{'}n \tag{3}$$

where $v_{\mathrm{f}}^{'}$ is the critical feed rate, $A^{'}$ is the actual ultrasonic amplitude, and n is the spindle speed.

Therefore, in the process of rotary ultrasonic drilling, if the spindle speed n is constant, the actual ultrasonic amplitude can be increased by increasing the excitation voltage, and the critical feed rate then increases, resulting in a higher feed rate when the cutting force sharply increases This is the reason why sharp increases appeared in the curves of 12 μm and 18 μm; in contrast, there was no sharp increase the curve of 24 μm, as the critical feed rate was not reached due of the larger amplitude. The results reveal the following.

1) Increasing the ultrasonic amplitude can effectively reduce the cutting force. Using the cutting force with a feed rate

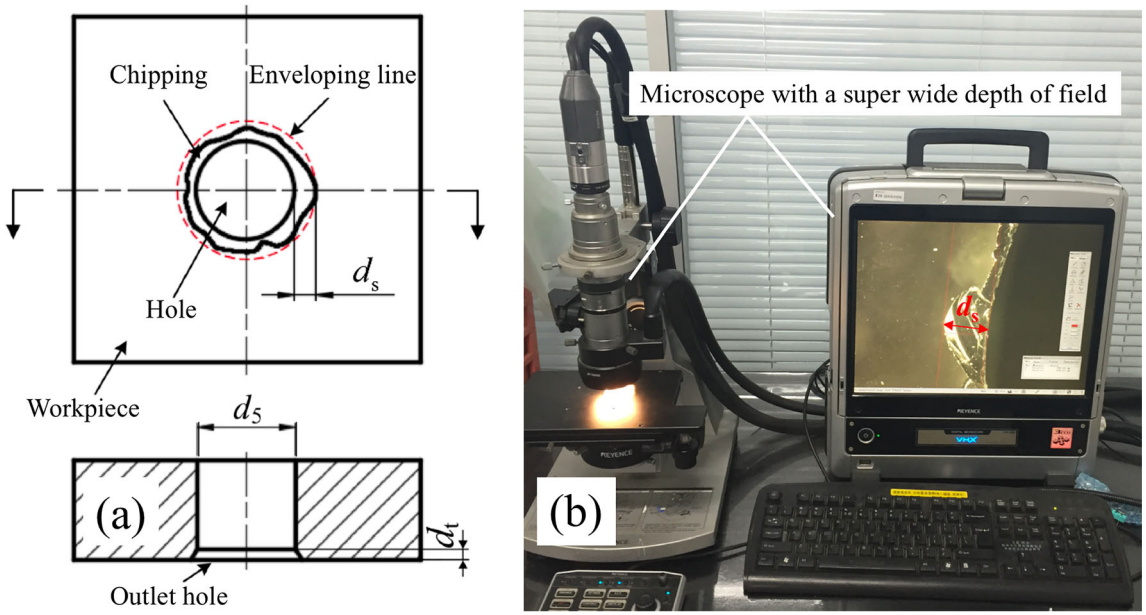

Fig. 10 Measurement schematic diagram for the edge-chipping size at the exit hole. **a** Measurement method. **b** Measurement instrument

of 6 mm/min as an example, compared with the traditional machining method (0 μm), the cutting force decreased by 47.2% when the ultrasonic amplitude was 12 μm. When the ultrasonic amplitude increased to 24 μm, the cutting force further decreased by 37.8%;

2) The sharp increase of the cutting force shows that the ultrasonic vibration was significantly suppressed, and the advantages of the GMRUMT were reduced. Increasing the ultrasonic amplitude can improve the feed rate when the cutting force sharply increases which means that the critical feed rate of the GMRUMT can be increased by using a larger amplitude.

4.3 Edge chipping at the exit hole

Figure 15 presents the effect of ultrasonic amplitude on the edge-chipping size at the exit hole in rotary ultrasonic drilling. From a physics perspective, a large amplitude produces higher impact force , and cracks will increase in proportion to the applied amplitude. However, from the viewpoint of the intermittent impact of rotary ultrasonic machining, the edge-chipping model can be obtained as follows [4]:

$$d_S^{\kappa} = \zeta H_V^{\frac{1}{10}} E^{\frac{1}{6}} K_{IC}^{-\frac{4}{3}} A'^{\frac{8}{15}} F_Z^{\frac{16}{15}} \tag{4}$$

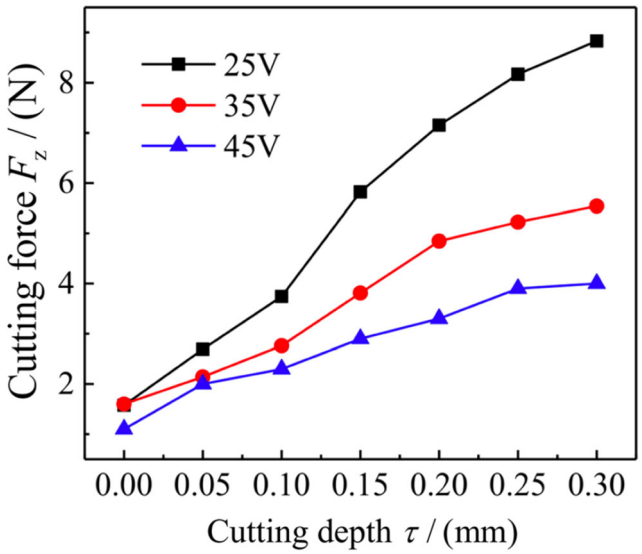

Fig. 11 Relationship between cutting force and cutting depth in ultrasonic face milling. (Spindle speed, 2000 r/min; feed rate, 80 mm/min)

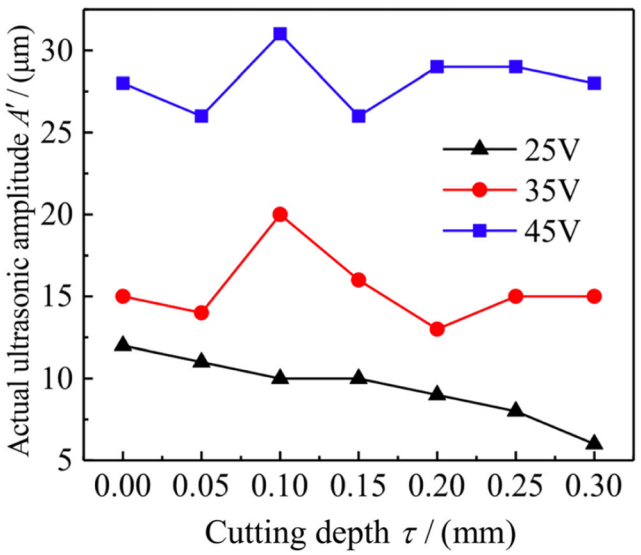

Fig. 12 Relationship between actual ultrasonic amplitude and cutting depth in ultrasonic face milling. (Spindle speed, 2000 r/min; feed rate, 80 mm/min)

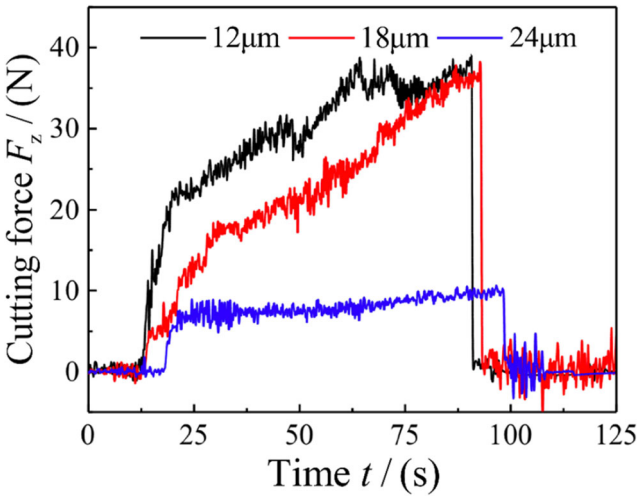

Fig. 13 Cutting force characteristics in ultrasonic drilling. (Spindle speed, 2000 r/min; feed rate, 4 mm/min)

where d_S is the size of the edge chip, κ is an exponent coefficient, H_V, E, and K_{IC} are the micro hardness, elastic modulus, and fracture toughness, respectively, and ζ is a proportionality constant that is independent of the cutting force, material properties, and κ.

In Equation (4), the dimension d_S is proportional to A' and F_Z. According to Fig. 13, the cutting force decreases with an increase in the ultrasonic amplitude. Therefore, the size of the edge chip d_S cannot be improved by using a large amplitude in theory; however, compared with the results without ultrasonic vibration (0 μm), the size of the edge chip was notably improved by using ultrasonic vibration.

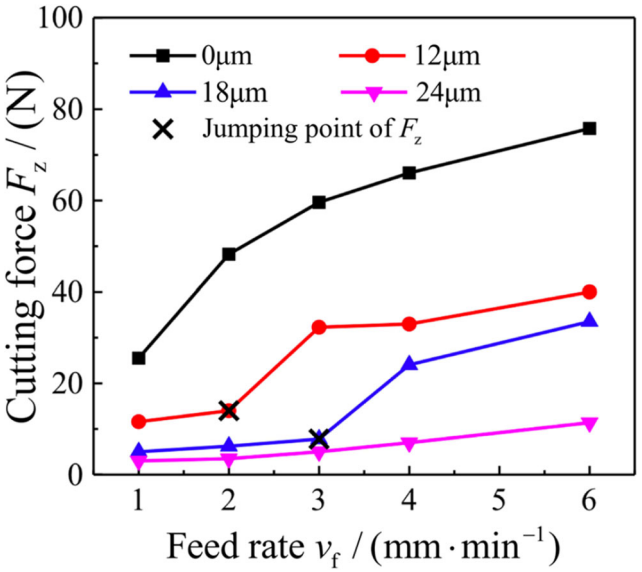

Fig. 14 Relation of cutting force and feed rate in ultrasonic drilling. (Spindle speed, 2000 r/min)

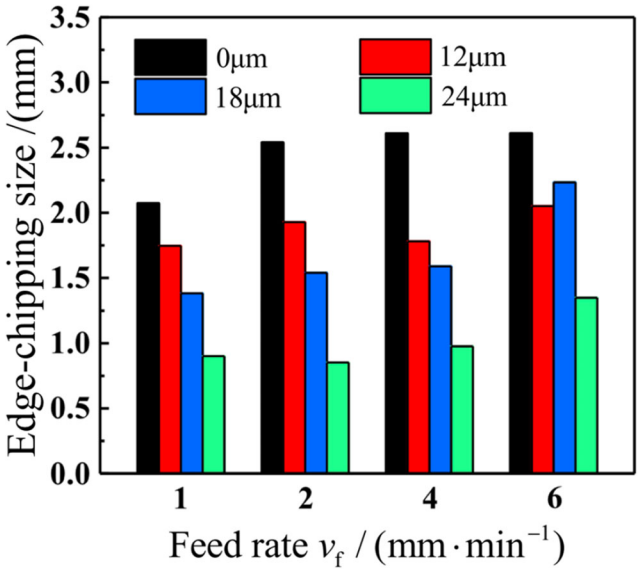

Fig. 15 Effect of ultrasonic amplitude on edge chipping at the exit hole. (Spindle speed, 2000 r/min)

4.4 Resonant frequency tuning

In the process of rotary ultrasonic drilling, the existing research has showed that the load will cause the increase of the resonant frequency of the system [30], therefore, this part aims to conduct the feasibility experiments of resonant frequency tuning in large amplitude GMRUMT, exploring the influence on machining process with or without tuning. In the cutting process, the excitation frequency was slowly increased in increments of 1 Hz via manual adjustment, and the result of the resonant frequency drift compensation was obtained at a certain degree, and the result was compared to those without tuning.

Figure 16a shows the effect of tuning on cutting force under two feed rates (1 mm/min and 2 mm/min) and three idling amplitudes (12 μm, 18 μm, and 24 μm). The percentages in the figure refer to the reduction ratios of the cutting force before and after tuning. It is evident that: (1) tuning can effectively reduce the cutting force under different ultrasonic amplitudes and cutting parameters and (2) tuning has a more significant effect on the cutting force when the ultrasonic amplitude is small. The reason for this is that the cutting force is greater under the condition of a small amplitude, which results in an increase in the resonant frequency drift of the system. Thus, the tuning effect is more significant.

Figure 16b shows the effect of tuning on the edge-chipping size at the exit hole at two feed rates (1 mm/min and 2 mm/min) and three ultrasonic amplitudes (12 μm, 18 μm, and 24 μm). The percentages in the figure refer to the reduction ratios of the edge-chipping size before and after tuning. When the ultrasonic amplitude was small, the effect of tuning on the edge-chipping damage was more significant. Based on the preceding research, tuning is of great significance for

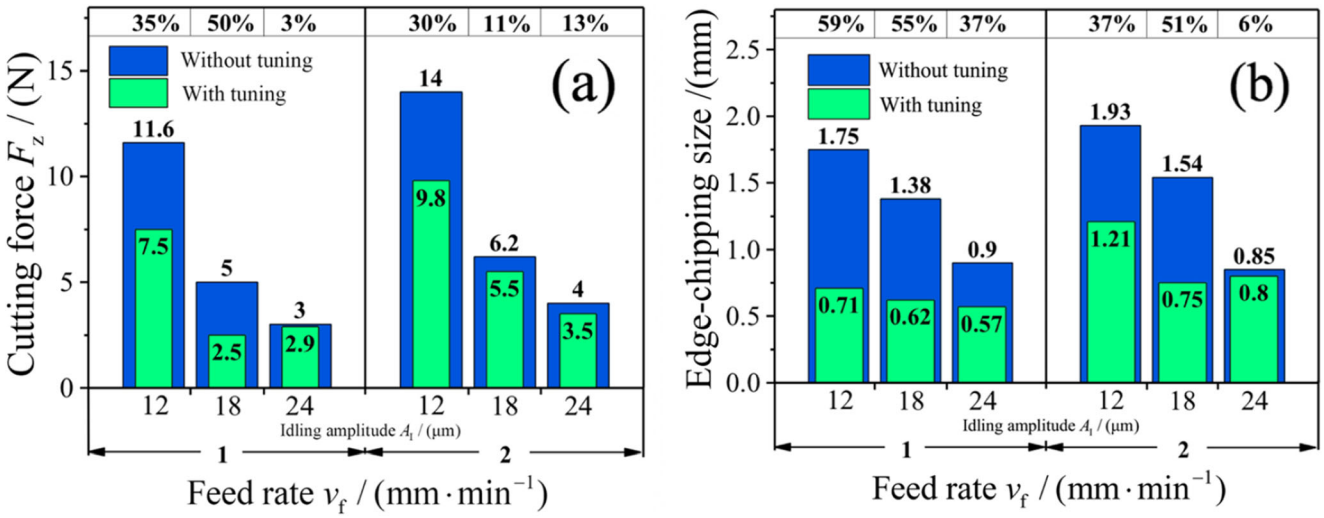

Fig. 16 Effect of tuning on machined quality. **a** Cutting force. **b** Edge chipping. (Spindle speed, 2000 r/min)

improving the actual ultrasonic amplitude, reducing the cutting force and edge-chipping damage, and improving the performance of the GMRUMT.

4.5 Tool wear

As presented in Fig. 17, it is evident that: (1) the cutting force clearly exhibited three stages of tool wear without ultrasonic vibration (0 μm), namely the initial wear stage, normal wear stage, and severe wear stage. When the number of holes was 32, the cutting force increased rapidly, which indicates that the tool life had been reached at this time; (2) in the process of small amplitude rotary ultrasonic drilling (12 μm or 18 μm), the cutting force increased slowly with the increase of the number of holes. When the number of holes was 36, the cutting force did not increase significantly, and the tool did not reach the wear limit, which indicates that the rotary ultrasonic drilling can be serviceable, effectively improving tool life; (3) in the process of large amplitude ultrasonic vibration machining (24 μm), the cutting force at all numbers of drilled holes was very stable, and there was no significant change, which indicates that the wear rate of the tool was slow, and the tool state was well-maintained.

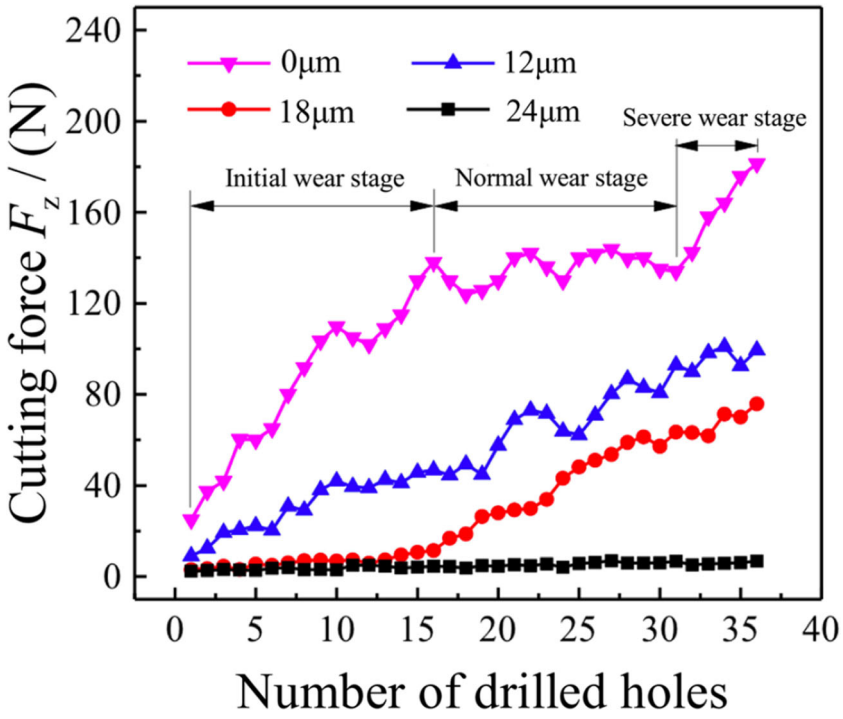

Fig. 17 Change of cutting force in tool wear process. (Spindle speed, 2000 r/min; feed rate, 2 mm/min)

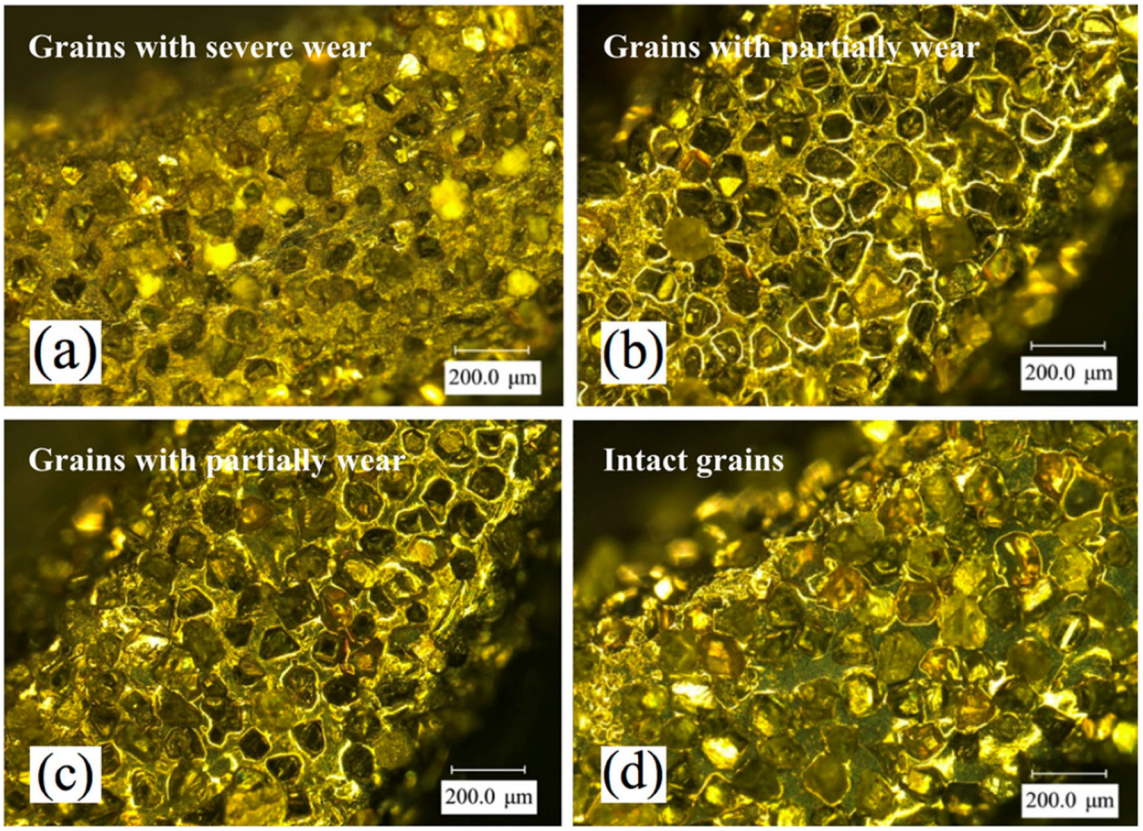

Fig. 18 The surface morphologies at the end faces of the tools. **a** $A = 0$ μm. **b** $A = 12$ μm. **c** $A = 18$ μm. **d** $A = 24$ μm. (Spindle speed, 2000 r/min; feed rate, 2 mm/min)

At the same number of machined holes (36), the final surface morphologies of the four tools were observed using the microscope with a super wide depth of field, as shown in Fig. 18 (the magnification is 100×).

In order to evaluate the tool wear qualitatively, the surface morphologies at the end faces of the tools under four ultrasonic amplitudes were observed. It can be seen from the figure that when the ultrasonic amplitude was 0 μm, the abrasive grains were severely worn; when the ultrasonic amplitude was 12 μm or 18 μm, the abrasive grains were partially worn; when the ultrasonic amplitude reached 24 μm, the abrasive grains remained intact, prolonging the tool life.

5 Conclusion

In this study, a GMRUMT with a large amplitude, high power, and stable amplitude output was developed. Via rotary ultrasonic face milling and rotary ultrasonic drilling experiments, the performance evaluation of the GMRUMT was conducted, and the conclusions are drawn as follows:

1) For a given voltage excitation, the GMRUMT proposed in this study exhibits a larger and more stable ultrasonic amplitude than the piezoelectric ultrasonic system at the same diameter of the transducers; it is also better suited for miniaturization due to the high power.
2) A large increase in the amplitude effectively reduces the axial mechanical load of the GMRUMT under certain machining parameters, resulting in the increased stability of the actual ultrasonic amplitude in the machining process; therefore, the edge-chipping damage in the machining process of brittle materials is reduced, and the machined quality is improved by using a large amplitude. Moreover, the critical feed rate of the GMRUMT is increased, optimizing the machining parameters. In addition, the tool wear is mitigated, thereby prolonging the tool life.
3) The tuning of the GMRUMT under machining load can help to improve the actual ultrasonic amplitude and the stability of the ultrasonic amplitude in the process of machining, thus reducing the cutting force and edge-chipping damage, and improving the performance of the GMRUMT.

Funding information The authors gratefully acknowledged the financial support for this research provided by the National Natural Science Foundation of China (Grant No. 51761145103 and Grant No. 51875311) and Shenzhen Foundational Research Project (Subject Layout) (Grant No. JCYJ20160428181916222).

Compliance with ethical standards

Conflict of interest The authors declare that they have no conflict of interest.

References

1. Arif M, Zhang X, Rahman M, Kumar S (2013) A predictive model of the critical undeformed chip thickness for ductile-brittle transition in nano-machining of brittle materials. Int J Mach Tool Manu 64(4):114–122. https://doi.org/10.1016/j.ijmachtools.2012.08.005
2. Inasaki I (1987) Grinding of brittle materials. CIRP Ann Manuf Technol 36(2):463–471. https://doi.org/10.1016/S0007-8506(07)60748-3
3. Diaz OG, Axinte DA (2017) Towards understanding the cutting and fracture mechanism in ceramic matrix composites. Int J Mach Tools Manuf 118–119:12–25. https://doi.org/10.1016/j.ijmachtools.2017.03.008
4. Wang J, Feng P, Zhang J, Zhang C, Pei Z (2016) Modeling the dependency of edge chipping size on the material properties and cutting force for rotary ultrasonic drilling of brittle materials. Int J Mach Tool Manu 101:18–27. https://doi.org/10.1016/j.ijmachtools.2015.10.005
5. Zhang C, Cong W, Feng P, Pei Z (2014) Rotary ultrasonic machining of optical K9 glass using compressed air as coolant: a feasibility study. Proc Inst Mech Eng B J Eng Manuf 228(4):504–514. https://doi.org/10.1177/0954405413506195
6. Churi N, Pei Z, Shorter D, Treadwell C (2009) Rotary ultrasonic machining of dental ceramics. Int J Mach Mach Mater 6(3–4):270–284. https://doi.org/10.1504/ijmmm.2009.027328
7. Wang J, Feng P, Zhang J, Ping G (2018) Experimental study on vibration stability in rotary ultrasonic machining of ceramic matrix composites: cutting force variation at hole entrance. Ceram Int: S0272884218311751. https://doi.org/10.1016/j.ceramint.2018.05.048
8. Chen J, Fang Q, Ping L (2015) Effect of grinding wheel spindle vibration on surface roughness and subsurface damage in brittle material grinding. Int J Mach Tool Manu 91:12–23. https://doi.org/10.1016/j.ijmachtools.2015.01.003
9. Zhang C, Rentsch R, Brinksmeier E (2005) Advances in micro ultrasonic assisted lapping of microstructures in hard–brittle materials: a brief review and outlook. Int J Mach Tool Manu 45(7):881–890. https://doi.org/10.1016/j.ijmachtools.2004.10.018
10. Xing Y, Deng J, Zhang G, Wu Z, Wu F (2017) Assessment in drilling of C/C-SiC composites using brazed diamond drills. J Manuf Process 26:31–43. https://doi.org/10.1016/j.jmapro.2017.01.006
11. Liu Y, Wang C, Li W, Zhang L, Yang X, Cheng G, Zhang Q (2014) Effect of energy density and feeding speed on micro-hole drilling in C/SiC composites by picosecond laser. J Mater Mach Technol. https://doi.org/10.1016/j.jmatprotec.2014.07.016
12. Abbas NM, Solomon DG, Bahari MF (2016) A review on current research trends in electrical discharge machining (EDM). Int J Mach Tool Manu 47(7):1214–1228. https://doi.org/10.1016/j.ijmachtools.2006.08.026
13. Hocheng NH, Liu CS (2000) Assessment of ultrasonic drilling of C/SiC composite material. Compos A 31(2):133–142. https://doi.org/10.1016/S1359-835X(99)00065-2
14. Kai D, Fu Y, Su H, Cui F, Li Q, Lei W, Xu H (2017) Study on surface/subsurface breakage in ultrasonic assisted grinding of C/SiC composites. Int J Adv Manuf Technol 91(9):1–11. https://doi.org/10.1007/s00170-017-0012-z
15. Yan W, Sarin VK, Lin B, Li H, Gillard S (2016) Feasibility study of the ultrasonic vibration filing of carbon fiber reinforced silicon carbide composites. Int J Mach Tool Manu 101:10–17. https://doi.org/10.1016/j.ijmachtools.2015.11.003
16. Singh RP, Singhal S (2016) Rotary ultrasonic machining: a review. Adv Manuf Process 31(14):1795–1824. https://doi.org/10.1080/10426914.2016.1140188
17. Feng P, Wang J, Zhang J, Zheng J (2017) Drilling induced tearing defects in rotary ultrasonic machining of C/SiC composites. Ceram Int 43(1):791–799. https://doi.org/10.1016/j.ceramint.2016.10.010
18. Aspinwall TB, Wise DK, Lh M (1998) Review on ultrasonic machining. Int J Mach Tools Manuf 38(4):239–255. https://doi.org/10.1016/S0890-6955(97)00036-9
19. Cong WL, Pei ZJ, Sun X, Zhang CL (2014) Rotary ultrasonic machining of CFRP: a mechanistic predictive model for cutting force. Ultrasonics 54(2):663–675. https://doi.org/10.1016/j.ultras.2013.09.005
20. Wang J, Feng P, Zhang J (2016) Reduction of edge chipping in rotary ultrasonic machining by using step drill: a feasibility study. Int J Adv Manuf Technol 87(9–12):2809–2819. https://doi.org/10.1007/s00170-016-8655-8
21. Clark AE (1988) Magnetostrictive rare earth-Fe2 compounds. Ferromagn Mater 1:43–99. https://doi.org/10.1007/978-3-642-73263-8_6
22. Koon NC, Williams CM, Das BN (1991) Giant magnetostriction materials. J Magn Magn Mater 100(1–3):173–185. https://doi.org/10.1016/0304-8853(91)90819-V
23. Claeyssen F, Lhermet N, Letty RL, Bouchilloux P (1997) Actuators, transducers and motors based on giant magnetostrictive materials. J Alloys Compd 258(1–2):61–73. https://doi.org/10.1016/s0925-8388(97)00070-4
24. Cai W, Zhang J, Yu D, Feng P, Wang J (2017) A vibration amplitude model for the giant magnetostrictive ultrasonic machining system. J Intell Mater Syst Struct 29(4):574–584. https://doi.org/10.1177/1045389X17711818
25. Cai W, Zhang J, Feng P, Yu D, Wu Z (2016) A bilateral capacitance compensation method for giant magnetostriction ultrasonic machining system. Int J Adv Manuf Technol:1–9. https://doi.org/10.1007/s00170-016-9602-4
26. Cai W, Feng P, Zhang J, Wu Z, Yu D (2016) Effect of temperature on the performance of a giant magnetostrictive ultrasonic transducer. J Vibroeng 18(2):1307–1318
27. Feng P, Cai W, Yu D, Zhang J, Wu Z (2015) Amplitude stability of giant magnetostrictive ultrasonic vibrator and piezoelectric ultrasonic oscillator The 16th National Conference on special processing, Xiamen, China, pp 358-365
28. Zha H, Feng P, Zhang J, Yu D, Wu Z (2018) Material removal mechanism in rotary ultrasonic machining of high-volume fraction SiCp/Al composites. Int J Adv Manuf Technol 97(5–8):2099–2109. https://doi.org/10.1007/s00170-018-2075-x
29. Wang J, Feng P, Zhang J, Cai W, Shen H (2017) Investigations on the critical feed rate guaranteeing the effectiveness of rotary ultrasonic machining. Ultrasonics 74:81–88. https://doi.org/10.1016/j.ultras.2016.10.003
30. Zhou H, Zhang J, Feng P, Yu D, Wu Z (2019) An output amplitude model of a giant magnetostrictive rotary ultrasonic machining system considering load effect. Precis Eng 60:340–347. https://doi.org/10.1016/j.precisioneng.2019.07.005